

## Ductility and strength assessment of HSC beams with varying of tensile reinforcement ratios

Mohammad Mohammadhassani<sup>\*</sup>, Meldi Suhatrii<sup>a</sup>, Mahdi Shariati<sup>b</sup> and Farhad Ghanbari<sup>c</sup>

*Department of Civil Engineering, University of Malaya, Malaysia*

*(Received July 29, 2013, Revised November 2, 2013, Accepted November 24, 2013)*

**Abstract.** Nine rectangular-section of High Strength Concrete(HSC) beams were designed and casted based on the American Concrete Institute (ACI) code provisions with varying of tensile reinforcement ratio as ( $\rho_{min}$ ,  $0.2\rho_b$ ,  $0.3\rho_b$ ,  $0.4\rho_b$ ,  $0.5\rho_b$ ,  $0.75\rho_b$ ,  $0.85\rho_b$ ,  $\rho_b$ ,  $1.2\rho_b$ ). Steel and concrete strains and deflections were measured at different points of the beam's length for every incremental load up to failure. The ductility ratios were calculated and the moment-curvature and load-deflection curves were drawn. The results showed that the ductility ratio reduced to less than 2 when the tensile reinforcement ratio increased to  $0.5\rho_b$ . Comparison of the theoretical ductility coefficient from CSA94, NZS95 and ACI with the experimental ones shows that the three mentioned codes exhibit conservative values for low reinforced HSC beams. For over-reinforced HSC beams, only the CSA94 provision is more valid. ACI bending provision is 10 percent conservative for assessing of ultimate bending moment in low-reinforced HSC section while its results are valid for over-reinforced HSC sections. The ACI code provision is non-conservative for the modulus of rupture and needs to be reviewed.

**Keywords:** High Strength Concrete (HSC); ductility; tensile reinforcement ratio; compressive strain

### 1. Introduction

The technical and economical viability of HSC has made it as a much preferred material in the construction industry. Many researchers (Cucchiara *et al.* 2012, Hester *et al.* 1990, Mohammadhassani 2011a, Shah and Ahmad 1998) had studied the behaviour of HSC sections with a concrete strength higher than 41.4MPa. Researchers such as Ho and Zhou (2011), Wang *et al.* (1978), Ibrahim and MacGregore (1994), Fashing and French (1999) had investigated the bending parameters of HSC beams. HSC is more brittle than normal concrete. There is a need to investigate the ductility of HSC sections especially in areas seismically active. Seismic design requires large ductility for the absorption of seismic energy to prevent sudden failure or significant degradation of strength even after the yielding of tensile reinforcements. There have been many advancements

---

\*Corresponding author, Ph.D., E-mail: mmh356@yahoo.com

<sup>a</sup>Senior Lecturer

<sup>b</sup>Ph.D.

<sup>c</sup>Structural Engineer

in the area of seismic performance of concrete structures in the last three decades including the ductility design of HSC structures (Mohammadhassani *et al.* 2010, Denvind and Hoat 2010). These advancements are especially vital in the serviceability of important structures such as nuclear power plants, reservoirs and hospitals. The ACI-349 Code covers the design of such high risk concrete structures that are subjected to impact loads such as earthquakes and tsunamis. Safe ductile designs had not been fully realized during the 1992 Landers, 1994 Northridge and 1995 Kobe earthquakes as well as the Japan 2011's earthquake and tsunami that had damaged the nuclear power plants in the Fukushima prefecture. In general, the behaviour of HSC sections for ductile design needs more investigations. Shin *et al.* (1989) had tested a large number of small scale HSC model beams subjected to monotonic or cyclic flexure loading and examined the ductility coefficients under cyclic loading. Fang *et al.* (1994) had investigated the cyclic behaviour of HSC beams with lower amounts of flexural reinforcement. The study reported in this paper mainly explored the implications of using HSC and its effect on ductility of RC flexural members. With sufficient experimental data and comprehensive literature review, this study investigates the ductility coefficient versus the variable of the tensile reinforcement ratio of HSC sections. The tensile bar influences crack widths and deflection in concrete sections. Crack widths and deflections are two important serviceability factors for concrete structures such as nuclear power plants, reservoirs and hospitals. This paper will highlight the contribution from this research in recommending review of code provisions for HSC ductile design.

For the abovementioned purpose, using the ACI318-95 code provision, nine rectangular HSC beams were casted and divided into two groups, Group I and Group II. Group I consists of five low-reinforced HSC beams; these beams are namely B1, B2, B3, B4 and B5 with corresponding tensile reinforcement ratios of  $\rho_{min}$ ,  $0.2\rho_b$ ,  $0.3\rho_b$ ,  $0.4\rho_b$  and  $0.5\rho_b$ . Group II consist of four over-reinforced HSC beams; these beams are namely B6, B7, B8 and B9 with tensile reinforcement ratios of  $0.75\rho_b$ ,  $0.85\rho_b$ ,  $\rho_b$ ,  $1.2\rho_b$ . During the loading process, concrete strain on the vertical face, strain in the tensile reinforcements and deflection at four points along the beam's length were measured and recorded. Corresponding graphs showing load-deflection, moment-curvature, load-crack width and related tables were studied and concluded.

## 2. Materials and methods

The mix design included local aggregates with a maximum diameter of 9.5mm, Ordinary Portland Cement and silica fume. A superplasticizer was also used to improve the setting time and workability. The properties of steel bars are shown in Table 1 that were determined from a tensile test on a number of samples taken from each steel bar batch supplied.

Table 1 Bar specification

Used bar	$f_y$ (kg/cm <sup>2</sup> )	$F_u$ (kg/cm <sup>2</sup> )	Area (cm <sup>2</sup> )
$\Phi_8$	3150	6081	0.5024
$\Phi_{12}$	3159	4889	1.1304
$\Phi_{14}$	3981	6127	1.5386
$\Phi_{16}$	3606	5833	2.0096
$\Phi_{18}$	3736	5952	2.5434

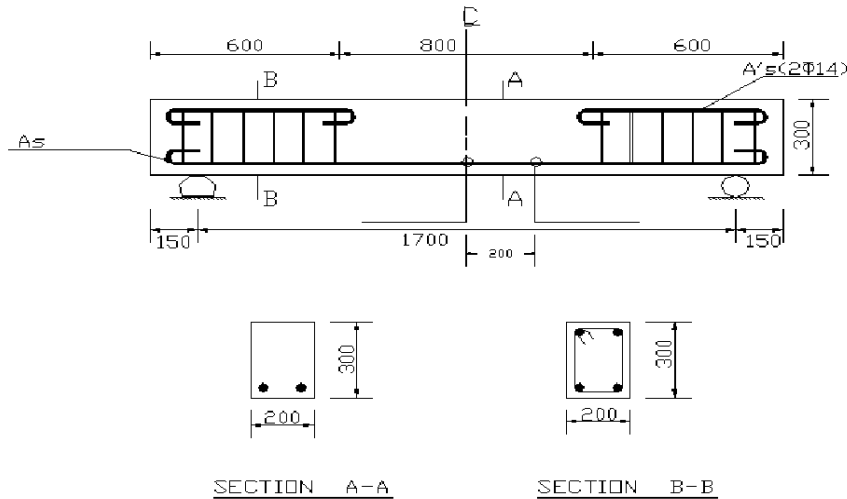


Fig. 1 Detail of casted beams

Table 2 The specification of tested beams

Beam's number	$f'_c$ (kgf/cm <sup>2</sup> )	$\rho$ (%)	$d$ (cm)	$A_s$ (cm <sup>2</sup> )
B1	670	0.61	25.6	3.08
B2	680	1.25	26.6	6.28
B3	675	2.03	25.8	10.20
B4	700	2.52	25.0	12.60
B5	700	3.05	25.0	15.20
B6	710	4.81	25.6	24.64
B7	705	5.39	26.6	28.66
B8	718	6.81	25.8	35.12
B9	725	8.01	25.0	40.04

The details of the HSC mixing process and the results of the material tests are described in Ghanbari and Mohammadhassani (2004). Fig. 1 shows geometrical details of casted beams.

The geometry specification for all the HSC beams was of 300mm depth, 200mm width and 2,000mm length.

The properties of hardened cementitious materials and the used tensile reinforcement ratio for each of casted beam are listed in Table 2.

The concrete strengths shown in Table 2 are the average of the cylinder compressive strengths of the samples at the age of loading for each beam.

The beams and samples were casted in steel moulds. The casted beams were demolded after 3 days and cured for two weeks. All nine simply supported HSC beams were loaded to ultimate capacity with a hydraulic jack. The experimental testing arrangement is shown in Fig. 2.

With each loading increment, the deflections were measured at four points with transducer gauges (LVDTs), the strain in the tensile bars was measured using electrical resistance gauges (ERGs) and the concrete strain was measured with mechanical Demec gauges. Fig. 2 shows the

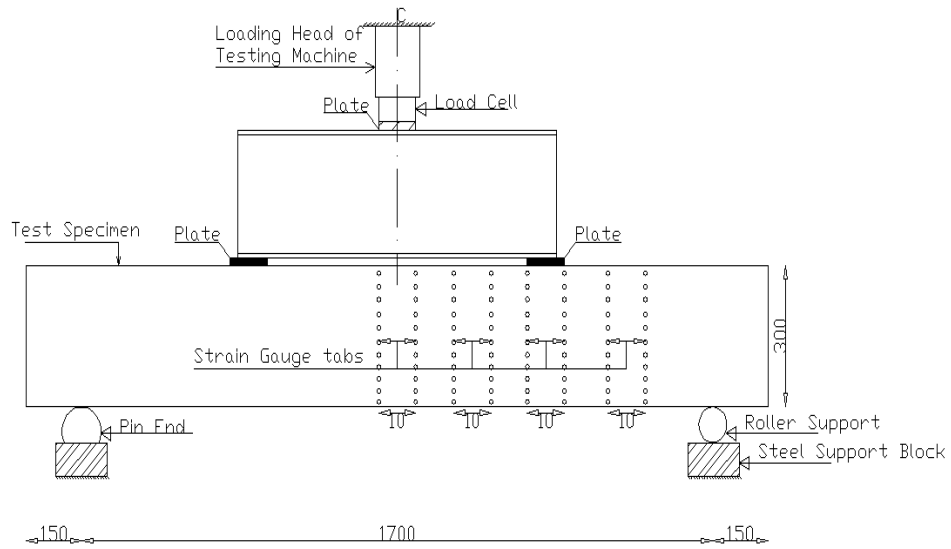


Fig. 2 Detail of testing arrangement

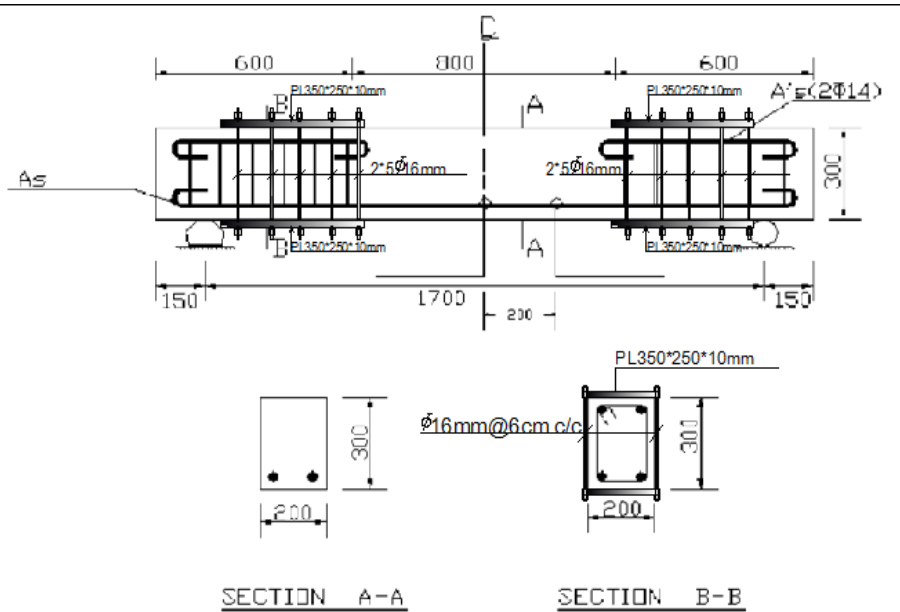


Fig. 3 Detail of beam (B7, B8 and B9)

positions of the transducers and Demec gauges in loading arrangement. The beams were subjected to increasing loads until failure occurred. At each loading step, data was gathered from the gauges to provide a comprehensive analysis. At each loading stage, the widths of the cracks were

measured with a hand-held microscope with an accuracy of 0.01mm. The strains and deflections were recorded for each of the nine beams using a data logger. Three of the beams namely B4, B5 and B6 failed in shear. External shear bars were used in B6, B7 and B8 to strengthen against shear failure (Fig. 3).

For beams that were destroyed in bending, the bending cracks first extended at mid-length of the beam; this is where the bending moment is maximum. The number of cracks and their widths increased with increasing loads. The propagation of the cracks was visually traced with the aid of a powerful lamp and marked accordingly. The corresponding loads were also recorded.

### 3. Results and discussion

The ductility of a RC member is the ability of the element or structural system to deform at or near the ultimate load without significant loss of strength. Ductility is a desired structural property because it allows stress redistribution and provides early warning signs of any impending failure. For ductile failure, a low-reinforced section is recommended so that the corresponding failure is initiated by the yielding of tensile bar after considerable deformation. This type of failure is ductile and is guaranteed by designing the RC beams with tensile reinforcement ratio substantially below the balanced ratio; ACI 318 requires at least 25 % below. This is where the steel yields and the concrete crushes simultaneously or reaches to its ultimate compressive strain. The reinforcement ratio thus provides a metric for ductility where the ductility corresponding to the maximum allowable reinforcement ratio provides a measure of the minimum acceptable ductility. Sometimes due to architectural considerations, it is not possible to enhance the dimension of a section to fulfil the allowable stress. The designer has to use an over-reinforced section where the failure is suddenly failing with concrete crushing and without any prior warning signs, e.g., deflection or visible cracks. This type of failure is brittle; any such design is not safe especially in earthquake prone areas where all codes require a ductile design. The main ductility parameters that represent the ductility index in bending sections are displacement and curvature.

In this regard, the deflection at the mid-span of the beam's length and the strain within the central pure bending zone were measured with a measuring tool. Data analysis, the load-deflection graph and the moment-curvature curve were drawn.

The ductility index based on the deflection was obtained as the ratio of maximum deflection to the yield deflection ( $\Delta_y$ ). Yield deflection ( $\Delta_y$ ) is the total deflection at mid-span when the first tensile bar yields. The maximum deflection  $\Delta_u$  was replaced with  $0.8(\Delta_{uf})$ , where  $\Delta_{uf}$  represents the ultimate amount of deflection when the fracture occurs. Thus, the ductility coefficient ( $\mu$ ) for all beams was computed based on the deflection and is presented in Table 3.

As seen in Table 3, increasing the tensile reinforcement ratio results lower ductility index. Except for the beams that failed in shear, the maximum ductility coefficient was observed in B1 with a tensile reinforcement ratio of  $\rho_{min}$  and the minimum ductility coefficient was observed in B9 with a tensile reinforcement ratio of  $1.2\rho_b$ . Although the tensile reinforcement ratio for B7 is more than that used in beams B4, B5 and B6 (refer to Fig. 4), its deflection ductility index is more in these three beams because B7 reached its ultimate moment capacity unlike beams B4, B5 and B6 which failed in shear before reaching their ultimate moment capacity.

Although In this study, shear design was carried out based on the ACI shear design provision, with the premature shear failure, Thus, it is necessary to review the shear design provision for HSC beams. To reach maximum ductility, it was important to consider the shear design provision

Table 3 Experimental ductility coefficient ( $\mu$ ) based on deflection index

Beam's number	$\rho$ (%)	$\Delta_y$ (mm)	$\Delta_{uf}$ (mm)	$\mu = \frac{\Delta_u^{**}}{\Delta_y}$	Failure mode
B1	0.61	3.59	43.18	9.600	bending
B2	1.25	5.99	40.99	5.470	bending
B3	2.03	5.59	20.10	2.870	bending
B4	2.52	7.76	15.40	1.580	shear
B5	3.05	N/A	N/A	N/A	shear
B6	4.81	9.29	9.70	1.045	shear
B7	5.39	6.96	12.84	1.845	bending
B8	6.81	8.77	14.00	1.597	bending
B9	8.01	9.43	12.52	1.327	bending

$\Delta_u^{**} = 0.8\Delta_{uf}$  N/A: not available



Fig. 4 The failure of beam B7

for the beams as bending fracture occurs before shear failure. Adequate shear capacity was therefore necessary to improve the ductile performance.

Extra shear bar was used in beams B7, B8 and B9 with external shear rehabilitation. The relation between the two sets of applied load and corresponding deflection are shown in Fig. 5.

As presented in Fig. 5, beams with higher tensile reinforcement ratio give a linear graph; this is indicative of a bending behaviour that is more elastic and is able to endure extra load with less deflection. This scenario is opposite to beams with lower tensile reinforcement ratios. By increasing of tensile reinforcement ratio, the ultimate load capacity increased but the deflection ductility index decreased.

Another method for investigating of ductility index for bending elements is based on curvature ( $\varphi$ ). The strains recorded were used to determine the curvature. The principle of curvature and neutral axis depth in RC beam sections is shown in Fig. 6.

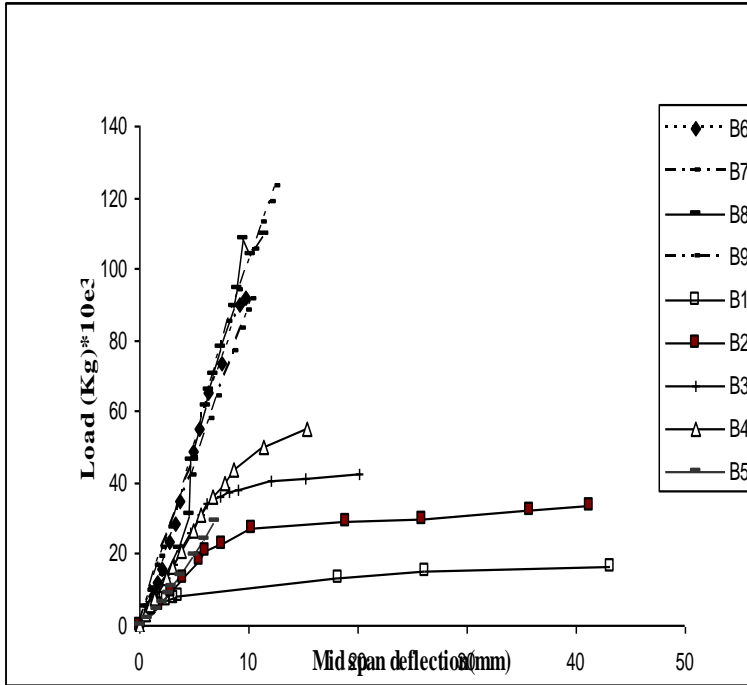


Fig. 5 Load-deflection curve

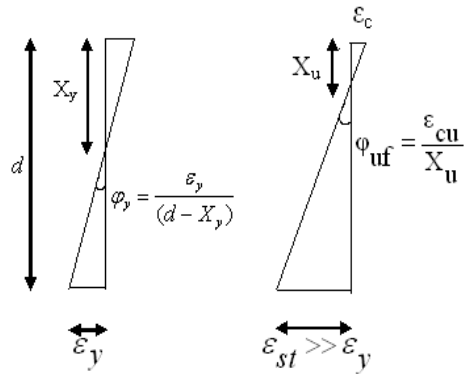


Fig. 6 Yield curvature ( $\phi_y$ ) and ultimate destructive curvature ( $\phi_{uf}$ ) in bending section

The ductility of a reinforced concrete section can be expressed in the form of the curvature ductility ( $\mu\phi$ ) as shown in Eq. (1)

$$\mu\phi = \mu = \frac{\phi_u}{\phi_y} \tag{1}$$

Table 4 Experimental ductility coefficient ( $\mu$ ) regarding curvature ( $\varphi$ )

Beam	$\rho(\%)$	$\Phi_y$	$\varphi_{\mu f}$	$\mu = \frac{\varphi_u^*}{\varphi_y}$
B1	0.61	0.0101	0.1200	9.500
B2	1.25	0.013	0.0870	5.350
B3	2.03	0.014	0.0735	4.200
B4	2.52	0.014	0.0466	2.660
B5	3.05	0.018	0.0270	1.200
B6	4.81	0.024	0.0260	1.083
B7	5.39	0.013	0.0230	1.779
B8	6.81	0.018	0.0250	1.406
B9	8.01	0.020	0.0280	1.428

$$\varphi_u^* = 0.8 \varphi_{\mu f}$$

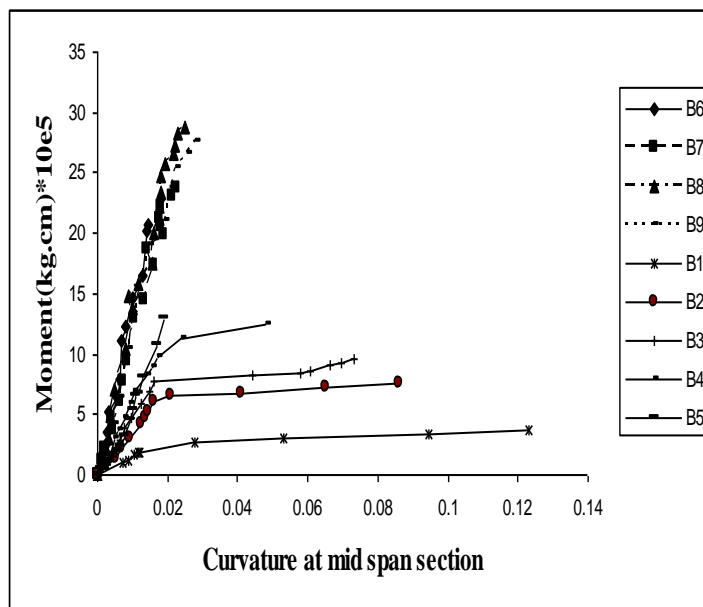


Fig. 7 Moment-curvature curve

$\varphi_u$  is the ultimate curvature where the compression strain of concrete reaches its ultimate value. It is assumed that at 80% of the failure load, thus  $\varphi_{\mu}$  is replaced with  $0.8(\varphi_{\mu f})$ .  $\varphi_{\mu f}$  represents the amount of curvature when fracture occurs and  $\varphi_y$  is the curvature amount when the tensile bar first reaches its yield strength. The experimental ductility coefficient ( $\mu$ ) based on curvature was calculated and presented in Table 4.

It can be deduced from Equation 1 that  $\mu\varphi \propto 1/\varphi_y$  thus a reciprocal influence of the steel bar's yield strength and that  $\mu\varphi \propto \varphi_u$  thus a direct influence on the effect of ultimate compression strain in concrete on ductility of RC beams.

As seen in Table 4, with the exception of the beams that failed in shear, all other beams showed a decrease in ductility coefficient as tensile reinforcement ratio increases. thus, it was observed that the tensile reinforcement ratio had the biggest influence on the curvature ductility index.

Fig. 7 confirms that the beams with lower tensile reinforcement ratio show initial elastic responses in their moment-curvature graphs that gradually decreases in stiffness till the ultimate moment is reached.

As seen in Table 4, in over-reinforced HSC Beams, the curvature ductility index is nearly constant, i.e., the HSC beams with tensile reinforcement ratio of more than  $0.75\rho_b$  have approximately the same flexural rigidity of the section (Fig. 7). In addition, it is observed that for over-reinforced HSC beams, the moment curvature curve is linear and elastic at all loading stages.

This finding justifies that the variation of curvature along the height of the section is influenced by the moment distribution and sectional stiffness of the specimen. The sectional stiffness is approximately constant or maintains a descending slope and, in addition, the neutral axis depth decreases slightly in the beams with a higher tensile reinforcement ratio after yielding of the tensile bar. A comparison of the curvature and displacement ductility shows approximately the same value for beams with a tensile reinforcement ratio of more than  $0.4\rho_b$ . This was also observed by Bernado & Lopes (2004) for beams with a high tensile reinforcement ratio.

The theoretical ductility coefficient is calculated regarding Eq. (2).

$$\mu = \varepsilon_{cu}(\alpha\beta_1f'_c)E_S(1 + \rho_n - (2\rho_n + \rho^2n^2)^{0.5}) / \rho f_y^2 \tag{2}$$

Table 5 shows the comparison of theoretical ductility coefficient that was calculated regarding Eq. (2) and presented based on the Canadian Standard Association (CSA 94), the 1995 New Zealand Concrete Standard (NZS95) and the ACI code provisions with the experimental ductility indexes.

Comparison of the experimental and theoretical ductility coefficients showed that the three aforementioned codes exhibit conservative values for the theoretical ductility coefficient of low-reinforced HSC beams. But for over-reinforced HSC beams, only the CSA94 provision is more

Table 5 Comparison of Experimental and theoretical ductility coefficients ( $\mu$ )

Beam's number	$\rho$ (%)	$\mu_{\Delta(\text{exp})}$	$\mu_{\phi(\text{exp})}$	$\mu_{(th)} \text{ACI}$	$\mu_{(th)} \text{CSA 94}$	$\mu_{(th)} \text{NZS95}$
B1	0.61	9.60	9.50	19.07	23.86	17.70
B2	1.25	5.47	5.35	8.26	10.33	7.67
B3	2.03	2.87	4.20	5.32	6.66	4.95
B4	2.52	1.58	2.66	3.66	4.57	3.40
B5	3.05	N.A	1.20	3.28	4.10	3.05
B6	4.81	1.045	1.083	1.49	1.38	1.87
B7	5.39	1.845	1.780	1.30	1.21	1.50
B8	6.81	1.597	1.410	1.15	1.07	1.40
B9	8.01	1.327	1.430	0.77	0.72	0.94

N.A=not available

Table 6 Comparison of theoretical and Experimental ultimate moment

Beam's number	$\rho$ (%)	$M_{u(\text{exp})}$ Kg.cm	$M_{u(\text{exp})}$ kg.cm	$M_{u(\text{exp})}/M_{u(\text{th})}$	Failure mode
B1	0.61	3.043e5	3.764e5	1.23	bending
B2	1.25	5.940e5	8.325e5	1.40	bending
B3	2.03	8.794e5	10.44e5	1.18	bending
B4	2.52	11.39e5	12.46e5	1.09	shear
B5	3.05	12.30e5	15.07e5	1.22	shear
B6	4.81	20.89e5	21.89e5	1.05	shear
B7	5.39	24.55e5	23.72e5	0.97	bending
B8	6.81	25.77e5	28.74e5	1.12	bending
B9	8.01	28.43e5	27.58e5	0.97	bending

\*Mean=1.14 & SD=0.017

Table 7 Predictions of ultimate moment for HSC beams

Researcher(s)	Number of beams studied	Range of $f'_c$ considered (Mpa)	$M_{u(\text{exp})}/M_{u(\text{th})}$	
			mean	Standard deviation
Rashid and Mansur (2005)	16	43 to 126	1.09	0.072
Ashour (2000)	9	49 to 102	1.02	0.032
Sarker <i>et al.</i> (1997)	13	65 to 91	1.07	0.097
Lin <i>et al.</i> (1992)	9	27 to 69	1.09	0.117
Lambotte and Taerwe (1990)	6	34 to 81	1.00	0.043
Shin(1989)	32	27 to 100	1.09	0.111
Pastor <i>et al.</i> (1984)	12	26 to 64	1.09	0.067
Lesliem Rajagopalan and Everard (1976)	12	64 to 81	1.16	0.146

valid. The  $\varepsilon_{cu}$  (the concrete strain at extreme compression fibre) is more than 0.0035; except for beams that have failed in shear, the resulting value of  $\varepsilon_{cu}$  for the HSC section is conservative by the ACI code provision but valid in terms of the CSA94 provision.

This part of the study provides experimental verification of the ultimate moment of a beam with rectangular cross-section subjected to pure bending. The experimental ultimate moment corresponding to the initiation of concrete crushing, is expressed as  $M_{u(\text{exp})}$ .

A comparison between the theoretical ultimate moment and the experimental ultimate moment in the tested HSC beams is shown in Table 6.

As noted in Table 6, the ACI code provision gives a conservative estimation for the ultimate moment capacity with a mean of 1.14 and a standard division of 0.017 for the ratio of  $M_{u(\text{exp})}$  to  $M_{u(\text{th})}$ . In addition, the ultimate moment increases as the tensile reinforcement ratio increases.

A comparison of the  $M_{u(\text{exp})}/M_{u(\text{th})}$  is tabulated in Table 7 with the findings of other researches such as Shin *et al.* (1989), Rashid and Mansur(2005), Sarker *et al.* (1997), Lin *et al.* (1992), Pastor *et al.* (1984), Lambotter and Taerwe(1990), Lesliem *et al.* (1976) .

The results of Table 7 confirm that the ACI code prediction in the ultimate bending strength of the HSC section is conservative by approximately 10 percent.

The Shape Factor, which is the ratio of the ultimate moment to the yield moment, provides an indication of the design efficiency. The yielding moment is the point at which the tensile bar

Table 8 Tensile bar strain, moment and concrete strain at extreme compression fibre (yielding condition)

The noted data at the moment of yielding bar condition.				
Beam's number	$\rho$ (%)	$M_Y$ (Kg.cm)	$\epsilon_{cy}$	$\epsilon_{sy}$
B1	0.61	1.874e5	0.00056	0.001924
B2	1.25	4.680e5	0.0012	0.002022
B3	2.03	6.930e5	0.0013	0.001990
B4	2.52	8.980e5	0.0016	0.001915
B5	3.05	12.930e5	0.0026	0.001859
B6	4.81	20.18e5	0.0039	0.001875
B7	5.39	14.45e5	0.0015	0.002018
B8	6.81	24.36e5	0.0027	0.001867
B9	8.01	21.09e5	0.0029	0.001830

Table 9 Shape factor of tested beams

The noted data at the moment of ultimate load (destructive condition).					
Beam's number	$\rho$ (%)	$M_u$ (Kg.cm)	$\epsilon_{cu}$	$E_{su}$	$M_{u(\text{exp})}/M_{y(\text{exp})}$
B1	0.61	3.764e5	0.00336	0.027416	1.62
B2	1.25	8.325e5	0.00342	0.018496	1.27
B3	2.03	10.44e5	0.00304	0.014821	1.27
B4	2.52	12.46e5	0.00315	0.008935	1.27
B5	3.05	15.07e5	0.00290	0.003800	0.95
B6	4.81	21.89e5	0.00410	0.001976	1.04
B7	5.39	23.72e5	0.00278	0.003017	1.69
B8	6.81	28.74e5	0.00380	0.002594	1.05
B9	8.01	27.58e5	0.00382	0.003217	1.34

ceases to behave elastically and permanent deformation occurs in order to sustain the applied load. The importance of the yield point is that any further increase in the moment causes drastic large increases in the curvature and deflection of the beam that may not be completely reversible when the load is removed.

The amounts of yielding & ultimate moment, concrete compressive strain and tensile strain are presented in Tables 8 and 9.

Table 9 shows that in over-reinforced HSC beams, the ratio of  $M_{u(\text{exp})}/M_{y(\text{exp})}$  is less than or closer to 1.0. This parameter shows a relative compatibility in the use of the general design equation for HSC section design as well as the larger average in low-reinforced HSC sections in comparison to over-reinforced HSC sections.

#### 4. Cracking moment

Cracking moment is the moment required for the first crack to occur at the extreme tension fibre. The importance of this index is that at this point the steel bar is exposed to the environment and may results in the corrosion of the steel. The control of the cracking in a Reinforced Concrete

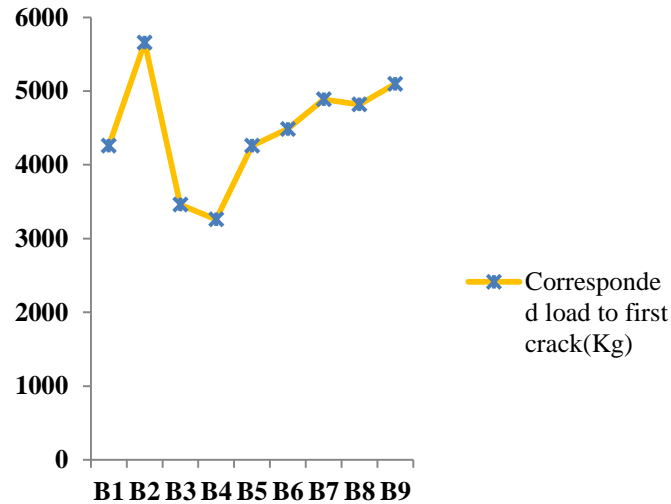


Fig. 8 Corresponded load to first crack

member is usually achieved by limiting the stress increment in the bonded reinforcement to some appropriately low value and ensuring that the bonded reinforcement is suitably distributed. For low-reinforced sections, depending on the grade of steel, yielding occurs immediately after cracking if the force in the member remains the same. Based on the experimental results shown in Fig. 8, the first crack happened at the extreme tension fibre at different loads for each beam.

The differences in Fig. 8 for the first crack load is dependent on parameters such as the cover of tensile bar, the number and size of tensile bar used and concrete strength at loading age. Combining the data in Fig. 8, Tables 10 and 11, a comprehensive attempt was made to determine the modulus of rupture. The cracking moment is presented as a function of the modulus of rupture in Eq. (3)

$$M_{cr} = \frac{f_r I_g}{y_t} \quad (3)$$

where

$f_r$  = The modulus of rupture of concrete.

$I_g$  = The moment of inertia of the gross section.

$y_t$  = the distance of the extreme tension fibre from the neutral axis.

The experimental cracking moments  $M_{cr,exp}$  are computed and compared with the ACI and CSA codes.

Based on Table 10 and Eq. (3), it is suggested that the modulus of rupture for a HSC section is as shown in Eq. (4)

$$f_r = 0.39\sqrt{f'_c} \text{ (Mpa)} \quad (4)$$

The ratio of the experimental cracking moment to the theoretical suggested with codes and researchers are presented in Table 11.

Table 10 Comparison of theoretical and Experimental cracking moment

Beam's number	$\rho$ (%)	$M_{cr(ACI)}$ Kg.cm	$M_{cr(CSA)}$ Kg.cm	$M_{cr(exp)}$ Kg.cm	$M_{cr(EXP)}/M_{cr(ACI)}$	$M_{cr(EXP)}/M_{cr(CSA)}$
B1	0.61	152250	73668.0	0.958e5	0.63	1.30
B2	1.25	153380	74215.0	1.273e5	0.83	1.72
B3	2.03	152810	73940.0	0.778e5	0.51	1.05
B4	2.52	155620	75300.0	0.734e5	0.47	0.97
B5	3.05	156620	75300.0	0.958e5	0.61	1.27
B6	4.81	156730	75835.0	1.010e5	0.64	1.33
B7	5.39	156170	75568.0	1.100e5	0.70	1.45
B8	6.81	157610	76261.4	1.0845e5	0.69	1.42
B9	8.01	158370	76630.0	1.148e5	0.72	1.49

Table 11 Predictions of cracking moment for HSC beams

Researcher's name	Number of beams	Considered parameters			$M_{cr,exp}/M_{cr,ACI}$		$M_{cr,exp}/M_{cr,rmp}$	
		Concrete strength $f'_c$ (MPa)	Tensile reinforcement ratio $\rho$ , (%)	Compressive reinforcement ratio $\rho'$ , (%)	Mean	Standard division	Mean	Standard division
Present study	9	67-72.5	0.61-8.01	0.4	0.64	0.102	0.87	0.021
Rashid and Mansur (2005)	16	43-126	1.25-5.31	0.31 and 0.94	0.90	0.126	0.62	0.083
Ashour (2000)	9	49-102	1.18-2.37	N/A *	1.02	0.131	0.69	0.124
Lambotte and taerwe (1990)	6	34-81	0.48-1.45	N/A *	0.77	0.207	0.57	0.192
Paulson <i>et al.</i> (1989)	9	37-91	1.49	0 to 1.49	0.68	0.114	0.49	0.118
Shin (2002)	28	27 to 100	0.41 to 3.60	0.41 to 3.60	1.00	0.216	0.71	0.190

Table 12 Comparison of modulus of rupture in various codes

Reference and authors	$f_r$ Mpa	$f_r$ ( $f'_c=70$ ) Mpa
ACI 318-95(1995)	$0.62 \sqrt{f'_c}$	5.18
ACI 363 (1984)	$0.97 \sqrt{f'_c}$	8.12
CSA94(1994)	$0.30 \sqrt{f'_c}$	2.51
shah and Ahmad (1998)	$0.42 (f'_c \cdot 150)^{0.68}$	7.58
Suggested equation	$0.39 \sqrt{f'_c}$	2.84

Table 12 presents the comparison of the modulus of rupture with those suggested with codes and other researchers.

It is noted that the suggested equation is very close to that by the CSA94 (Canadian Standards Association 1994) while the ACI code provision is non-conservative for the modulus of rupture.

The flexural cracks start from the tension face and propagate perpendicular to the axis of the member. The crack width of a flexural crack depends on parameters such as tensile stress in the

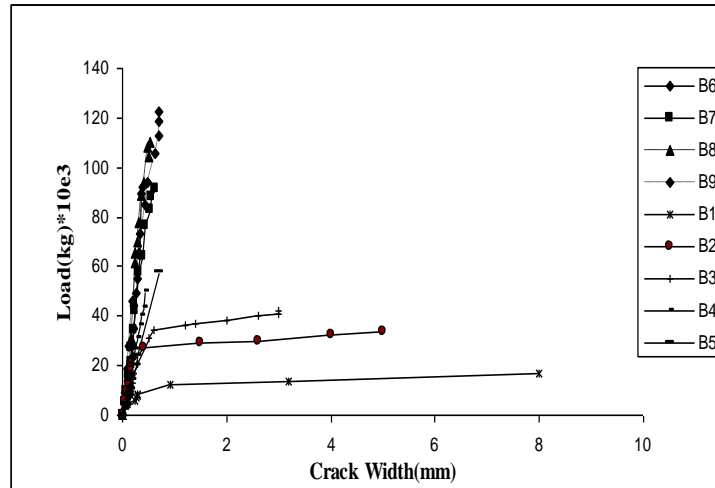


Fig. 9 Load-crack width curve

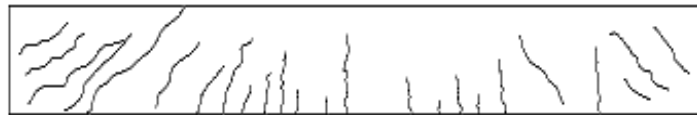


Fig. 10 Crack's progress in beam B6

longitudinal bars, thickness of the concrete cover, diameter and spacing of longitudinal bars, section depth, the location of the neutral axis, bond strength and the tensile strength of concrete.

For this study, The load-crack widths curves are presented in Fig. 9.

With increasing the applied load, the tensile cracks extend diagonally towards the loads and supports. A schematic of the occurrence and development of the cracks in the tested beams is available in Ghanbari and Mohammadhassani (2004). a sample of crack propagation in B6 is shown in Fig. 10.

The results indicate the relatively significant effect of tensile bar on the maximum crack width for over-reinforced HSC beams. All over-reinforced HSC beams collapsed in destructive loads with low crack widths. The effect of tensile bar on the beam's crack width is observed in over-reinforced HSC sections, where the increment in the neutral axis movement is slightly less (refer Fig. 4) than the low-reinforced HSC sections. However, in low-reinforced sections, the strain increases and the neutral axis depth moves rapidly upwards. These major differences relate to the design procedure as low-reinforced sections are designed to have the tensile bar yielding before the concrete crushing but over-reinforced act to have the concrete crushing before the tensile bar yields.

## 5. Conclusions

Nine HSC beams of varying tensile reinforcement ratio were casted and loaded to study the effect of tensile reinforcement ratio on the ductility of HSC sections.

The linear graphs between the applied load and corresponding deflection or curvature in over-reinforced HSC beams show that the behaviour of these beams is elastic and any increase in the tensile reinforcement ratio results increasing in the ultimate load too.

For the low-reinforced HSC sections, the moment-curvature graph and load-deflection curve start with an initial elastic response followed by an inelastic behaviour that appears with a gradual decrease in the stiffness till the ultimate moment is reached. However, when the ductility decreases slightly, it shows a nearly constant stiffness and minor changes in the neutral axis depth after the bar yields. In addition, the curvature and displacement ductility indexes show approximately the same value for HSC sections with a tensile reinforcement ratio more than  $0.4\rho_b$ .

The comparison of the experimental and theoretical ductility coefficient based on the Canadian Standard Association (CSA 94), the 1995 New Zealand Concrete Standard (NZS95) and ACI shows that the three mentioned codes exhibit conservative amounts of theoretical ductility coefficient for low-reinforced sections. For over-reinforced HSC sections, only the CSA94 provision is valid.

The practical value for the concrete strain at extreme compression fibre is  $\varepsilon_{cu} > 0.0035$  except for the beams that have failed in shear. Therefore, the  $\varepsilon_{cu}$  value for the HSC section design in the ACI code provision is conservative and so the CSA94 provision is more applicable in this case.

Comparison of the theoretical and experimental ultimate bending moment shows that the ACI code provision in low-reinforced HSC section is 10 percent conservative but for over-reinforced HSC sections is valid.

The experimental amount of shape factor,  $M_{u(\text{exp})}/M_{y(\text{exp})}$ , shows a larger average in low-reinforced HSC sections in comparison with over-reinforced HSC sections. Therefore, based on this study, the design factors in ACI code provision need to be reviewed for low-reinforced HSC sections.

This study also suggests the modulus of rupture in HSC section to be  $f_r = 0.39\sqrt{f'_c}$  (Mpa). It is very close to CSA94 code provision; while the ACI code provision is non-conservative for the modulus of rupture.

Shear failure occurs before the ultimate moment capacity is achieved in over-reinforced HSC sections. To achieve maximum ductility, Thus, it is necessary to review the ACI shear provision for the designing of over-reinforced HSC beams.

## References

- ACI Committee 318 (1995), Building Code Requirements for Reinforced Concrete, (ACI 318-95) and Commentary, American Concrete Institute, Detroit.
- ACI Committee 363 (1984), State-of-the-Art Report on High Strength Concrete, *ACI Journal*, **81**(4), 364-399.
- American Concrete Institute, ACI 349-90, Code Requirements for Nuclear Safety Related Concrete Structures.
- Ashour, S.A. (2000), "Effect of compressive strength and tensile reinforcement ratio on flexural behaviour of high-strength concrete beams", *Eng. Struct.*, **22**(5), 413-423.
- Bernardo, L.F.A. and Lopes, S.M.R. (2004), "Neutral axis depth versus flexural ductility in high strength concrete beams", *Struct. Eng.*, **130**(3), 452-459.
- CSA94 (1994), CSA Technical Committee, Design of concrete structure for buildings, CAN3-A23.3-M94, Canadian Standards Association, Rexdale, Ontario.
- Calogero, C., Marinella, F. and Maurizio, F. (2012), "Steel fibre and transverse reinforcement effects on the

- behaviour of high strength concrete beams”, *Struct. Eng. Mech.*, **42**(4), 551-570.
- Lau, D. and Pam, H.J. (2010), “Experimental study of hybrid FRP reinforced concrete beams”, *Eng. Struct.*, **32**, 3857-3865.
- Fang, I.K., Wang, C.S. and Hong, K.L. (1994), “Cyclic behaviour of high strength concrete short beams with lower amount of flexural reinforcement”, *ACI Struct. J.*, **91**(1), 10-18.
- Fasching, C.J. and French, C.E. (1999), “Effect of high strength concrete (HSC) on flexural members and high strength concrete in seismic regions”, *ACI Int. J.*, 176.
- Ghanbari, F. (2004), “Analysis and design of high strength concrete beams with low tensile reinforcement ratio in seismic hazard area”, Civil Engineering Department, Kerman University.
- Hester, W.T. (1990), *High-Strength Concrete-Second International Symposium*, SP-121, American Concrete Institute, Farmington Hills, Mich.
- Ho, J.C.M. and Zhou, K.J.H. (2011), “Concurrent flexural strength and deformability design of high-performance concrete beams”, *Struct. Eng. Mech.*, **40**(4), 541-562.
- Ibrahim, H.H.H and MacGregore, J.G. (1994), “Flexural behaviour of high strength concrete columns”, Structural Engineering Report, No.196, 97.
- Lambotte, H. and Taerwe, L.R. (1990), “Deflection and cracking of high strength concrete beams and slabs”, *High-strength concrete, Second International Symposium*, SP-121, Ed. Hester, W.T., American Concrete Institute, Farmington Hill, Mich.
- Leslie, K.E., Rajagopalan, K.S. and Everard, N.J. (1976), “Flexural behaviour of high strength concrete beams”, *ACI J.*, **73**(9), 517-521.
- Lin, C.H., Ling, F.S. and Hwang, C.L. (1992), “Flexural behaviour of high strength fly ash concrete beams”, *J. Chin. Ins. Eng.*, **15**(1), 85-92.
- Mohammadhassani, M. (2004), “Analysis and design of over-reinforced high strength concrete beams in seismic hazardous area”, Civil Engineering Department, Kerman University.
- Mohammadhassani, M., Jumaat, M.Z. and Jameel, M. (2010), “Experimental study on ductility of high strength reinforced concrete beams with low longitudinal tensile reinforcement ratio for seismic hazardous areas”, *International Conference on Sustainable building and infrastructure (ICSBI2010)*, Kuala Lumpur Convention Centre, June.
- Mohammadhassani, M., Chemrouk, M. and Jameel, M. (2011a), “An experimental investigation on bending stiffness and neutral axis depth variation of over-reinforced high strength concrete beams”, *Nucl. Eng. Des.*, 2060-2067.
- Pastor, J.A., Nilson, A.H. and Slate, F.Q. (1984), “Behaviour of high strength concrete beams”, Research Report No. 84-3, Department of Structural Engineering, Cornell University, Ithaca, N.Y.
- Paulson, K.A., Nilson, A.H. and Hover, K.C. (1989), “Immediate and long-term deflection of high strength concrete beams”, Research Report No. 89-3, Department of Structural Engineering, Cornell University, Ithaca, N.Y..
- Rashid, M.A. and Mansour, M.A. (2005), “Reinforced high strength concrete beams in flexure”, *ACI Struct. J.*, **102**(3), 462-471.
- Sarker, S., Adwan, O. and Munday, J.G.L. (1997), “High strength concrete an investigation of the flexural behaviour of high strength beams”, *Struct. Eng.*, **75**(7), 115-121.
- Shah, S.P. and Ahmad, S.H. (1998), *High performance concrete: Properties and applications*, McGraw Hill.
- Shin, S.W., Ghosh, S.K. and Moreno, J. (1989), “Flexural ductility of ultra-high-strength concrete members”, *ACI Struct. J.*, **86**(4), 394-400.
- Shin, S.W., Mansur, M.A. and Paramasivam, P. (2002), “Correlations between mechanical properties of high strength concrete”, *J. Mater. Civil Eng.*, ASCE, **14**(3), 230-238.
- Wang, P., Shah, S.P. and Naaman, A.E. (1978), “High strength concrete in ultimate strength design”, *ASCE J. Struct. Div.*, **104**(11), 1761-1773.